(Received 24 December 2024, Accepted 10 January 2025, Scheduled 18 February 2025)

Novel Hexagonal Cross-Coupled Dielectric Waveguide Filter

Xiaotao Yao[1], Yunxiu Wang[1,*], Yang Gao[1], and Jiankang Zhang[2]

[1]School of Electronic and Information Engineering, China West Normal University, Nanchong 637009, China
[2]School of Electronics and Information, Hangzhou Dianzi University, Hangzhou 310018, China

ABSTRACT: In this paper, a six-order cross-coupled ceramic dielectric waveguide filter (CDWF) based on equilateral triangle resonators is introduced. It is composed of a regular hexagonal cavity, which is divided into six equilateral triangular blocks. The filter exhibits two transmission zeros outside the passband that ensure its out-of-band suppression greater than 45 dB. Measured results show that the insertion loss is less than 1 dB and the return loss more than 16 dB within the operating frequency range of 3.4–3.6 GHz. The ceramic dielectric used here has a dielectric constant of 20.3 and a thickness of 5 mm. Thus, it has the advantages of compact size and excellent frequency selectivity.

1. INTRODUCTION

With the rapid development of 5G communication and the continuous innovation of ceramic dielectric process in recent years, ceramic dielectric waveguide filters (CDWFs) are playing an important role in modern wireless communication systems because of their high temperature stability, corrosion resistance, compact size, and light weight. As a result, CDWFs have gained increasingly interest and industry research [1–6]. Compared to other structures, rectangular CDWFs are the most widely used due to their relatively mature technology. At present, the block is usually separated into several interconnecting independent resonators by rectangular [1], T-shaped [2], or cross holes [3] isolation windows. The couplings among these resonators are also achieved through these holes. In addition, to facilitate mediation of the single-cavity frequency towards the center frequency, a coupling blind hole is often introduced. Although rectangular CDWFs have some advantages, their sizes are relatively large. Therefore, many scholars have attempted to study other structures. For example, the authors in [4] proposed a CDWF based on isosceles right-angled triangular resonators which was proved to be miniaturized and suitable for high power applications. In [5], a 5-order CDWF was presented base on cylindrical dielectric resonators, which possesses the advantages of small insertion loss, small size, and good rejection out of passband. Additionally, [6] concerns a CDWF composed of 90-degree sectorial resonators, which exhibits excellent property, for example, a high Q value and miniaturization.

In this paper, a CDWF is designed routinely using equilateral triangular resonators. By introducing coupling windows from the center to six corners on a whole hexagonal ceramic dielectric block, a hexagonal sixth-order cross-coupled dielectric waveguide filter is realized. The designed filter exhibits the following performance metrics: insertion loss $\leq$ 1 dB, return loss $\geq$ 16 dB, a center frequency of 3.5 GHz, operational bandwidth of 200 MHz, out-of-band suppression $\geq$ 45 dB, and two out-of-band transmission zeros at 3.28 and 3.72 GHz.

2. ANALYSIS AND DESIGN

Currently, the exploration and design for dielectric waveguide filters are mainly focused on single-cavity resonator and the optimization of coupling topology. In this paper, a compact filter is designed with six equilateral triangular resonators.

Firstly, a Cartesian coordinate system of a equilateral triangular waveguide with its cross-section as depicted in Fig. 1 is established.

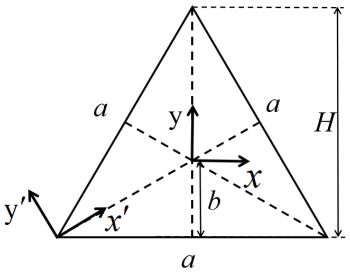

FIGURE 1. Equilateral triangular dielectric waveguide.

Given that the side length of this equilateral triangle is denoted as a, its height as H, and the radius of the inscribed circle as b, we can get

$$H = \frac{\sqrt{3}}{2}a = 3b \tag{1}$$

Now, translate and rotate the coordinate system to (x', y'). Referring to [7], for the TM wave, E_z can be defined by Equation (2).

$$E_Z = \sin\frac{l\pi x'}{3b}\cos\frac{p\pi y'}{3\sqrt{3}b} + \sin\frac{m\pi x'}{3b}\cos\frac{q\pi y'}{3\sqrt{3}b} +$$

* Corresponding author: Yunxiu Wang (627662147@qq.com).

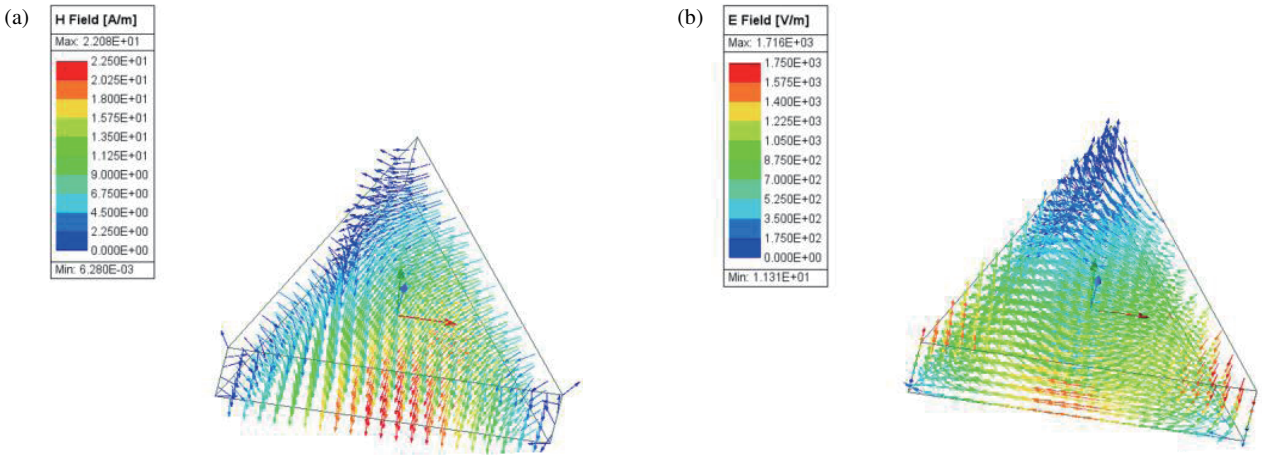

FIGURE 2. Distribution of electromagnetic fields. (a) Magnetic field. (b) Electric field.

$$+\sin\frac{n\pi x'}{3b}\cos\frac{r\pi y'}{3\sqrt{3}b} \tag{2}$$

where l, m, n, p, q, and r are integers, and the boundary conditions on two sides are taken into account.

$$E_Z|_{y'=\pm x/\sqrt{3}}=0 \tag{3}$$

If we set

$$\left.\begin{aligned} l-\frac{p}{3}+m+\frac{q}{3}&=0\\ m-\frac{q}{3}+n+\frac{r}{3}&=0\\ n-\frac{r}{3}+l+\frac{p}{3}&=0 \end{aligned}\right\} \tag{4}$$

it can be inferred that l, m, and n must adhere to the following relationship.

$$l+m+n=0 \tag{5}$$

Rotating (x, y) coordinates counterclockwise by 30 degrees, then moving the coordinate origin, as shown in Figure 1, we can obtain formula (6)

$$\begin{cases} x'=\dfrac{\sqrt{3}}{2}x+\dfrac{1}{2}y+2b\\ y'=-\dfrac{1}{2}x+\dfrac{\sqrt{3}}{2}y \end{cases} \tag{6}$$

If we apply the three coordinates u, v, and w in [8],

$$\begin{cases} u=\dfrac{\sqrt{3}}{2}x+\dfrac{1}{2}y\\ v=-\dfrac{\sqrt{3}}{2}x+\dfrac{1}{2}y\\ w=-y \end{cases} \tag{7}$$

Bringing the (7) into (2) will lead to

$$\begin{aligned} E_Z=&\sin\frac{2\pi l}{3b}\left(\frac{u}{2}+b\right)\cos\frac{\pi(m-n)(v-w)}{9b}\\ &+\sin\frac{2\pi m}{3b}\left(\frac{u}{2}+b\right)\cos\frac{\pi(n-l)(v-w)}{9b}\\ &+\sin\frac{2\pi n}{3b}\left(\frac{u}{2}+b\right)\cos\frac{\pi(l-m)(v-w)}{9b} \end{aligned} \tag{8}$$

$$k=\frac{2\pi}{3b}\sqrt{m^2+mn+n^2}=\frac{4\pi}{3a}\sqrt{m^2+mn+n^2} \tag{9}$$

k is the wave number.

For TM waves, l, m, and n cannot be zero, otherwise $E_Z=0$. Consequently, for the lowest wave mode of TM wave ($m=n=1$) we can get

$$k=\frac{2\pi}{\lambda}=\frac{4\pi}{a\sqrt{3}},\quad \lambda=3b=H \tag{10}$$

It can be obtained from $\lambda=\frac{c}{f\sqrt{\varepsilon_r}}$ that the resonant frequency of TM_{11} is

$$f_{\mathrm{TM}_{11}}==\frac{c}{\lambda\sqrt{\varepsilon_r}}=\frac{c}{H\sqrt{\varepsilon_r}}=\frac{c}{(\sqrt{3}a/2)\sqrt{\varepsilon_r}}\approx\frac{c}{0.87a\sqrt{\varepsilon_r}}$$

Thus

$$a=\frac{c}{0.87f_{\mathrm{TM}_{11}}\sqrt{\varepsilon_r}} \tag{11}$$

where ε_r is the dielectric constant, and c is the light speed in free space.

Subsequently, the analysis of the electromagnetic field distribution of the equilateral triangle resonator was conducted through simulation modeling, as depicted in Fig. 2, revealing that the main mode is TM_{11}.

Then, a single-cavity structure was designed as illustrated in Fig. 3. A blind hole with a diameter of d_1 and a depth of h_n was excavated at the center of the equilateral triangular waveguide mentioned above. The thickness of the dielectric block is h.

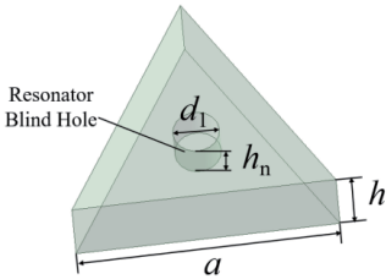

FIGURE 3. 3D model of the presented single-cavity.

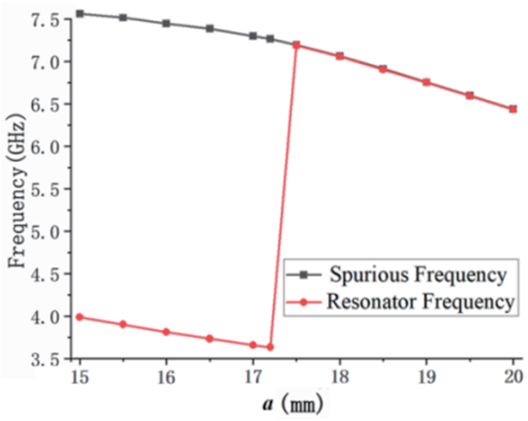

FIGURE 4. Curve of resonant frequency and spurious frequency with side length of the resonator.

Based on the center frequency of 3.5 GHz, the side length a can be calculated as 20 mm. However, considering the impact of blind holes, a should be slightly shortened to about 17.5 mm. As shown in Fig. 4, when a is around 17.2 mm, the resonant frequency is closest to the center frequency. Once a exceeds 17.2 mm, the resonant frequency changes dramatically, eventually causing the fundamental mode to overlap with higher-order modes.

The thickness of the ceramic embryo h and the depth of the tuning blind hole h_1 largely influence the resonant frequency of the filter. In Fig. 5, the resonant frequency does not vary much while the parasitic frequency drops sharply as the thickness of the dielectric (h) increasing. When $h = 5$ mm, the single-cavity resonant frequency converges most closely to the target center frequency. It is worth mentioning that the blind hole should not be too deep. Otherwise, it will be more difficult to adjust the resonance frequency. Fig. 6 shows the relationship between the resonant frequency and spurious frequency with the depth of the resonant blind hole (h_1). Obviously, with the increase of h_1, the spurious frequency is quite stable, while the resonant frequency changes significantly, and the two frequency curves coincide when the blind hole depth is equal to 2.4 mm. So h_1 is mainly determined by the resonant frequency, which is about 2.3 mm.

In Fig. 7, the entire hexagonal ceramic dielectric block is divided into six resonators by six slots with different lengths $l_{12} = l_{56}$, $l_{23} = l_{45}$, and the lengths of l_{34} and l_{16} are different. The widths of all these slots are $t = 1$ mm. Six resonant blind holes are set in the middle vertical line of the triangle at a distance of $L = 10$ mm from the center of the hexagon with different depths $h_1 \sim h_6$ and same diameter $d_1 = 3$ mm. At the same time, there are six coupling blind holes with the same diameter $d_2 = 2$ mm, different depths (h_{mn}) and locations from the center of the filter. The position of each coupling hole is located at the center from the endpoint of the middle slot to the hexagonal vertex [9].

In Fig. 8, the input and output ports are coaxial feed. Two feeder holes are respectively set in the opposite positions directly underneath resonator 1 and resonator 6. Their depths can be used to change the magnitude of the input-output coupling.

Higher out of band rejection with a lower number of elements may be achieved by introducing finite frequency transmission zeros [10]. The coupling topology structure of the filter is shown in Fig. 9. The negative coupling of resonators 3 and 4 is realized by the slot and the deep blind hole between them, while positive couplings of other remaining resonators are due to other slots and the shallow blind holes between 1 and 2, 2 and 3, 4 and 5, and so on. The coupling properties can be transformed by adjusting the depth of the coupling blind holes [11]. Thus, a sixth-order cross-coupling topology is realized [12]. The final coupling coefficients are shown in (12).

$$M = \begin{pmatrix} 0 & 1.016 & 0 & 0 & 0 & 0 & 0 & 0 \\ 1.016 & 0.029 & 0.877 & 0 & 0 & 0 & 0.0025 & 0 \\ 0 & 0.877 & 0.03 & 0.635 & 0 & 0 & 0 & 0 \\ 0 & 0 & 0.635 & 0.016 & -0.658 & 0 & 0 & 0 \\ 0 & 0 & 0 & -0.689 & 0.031 & 0.621 & 0 & 0 \\ 0 & 0 & -0.067 & 0 & 0.697 & 0.031 & 0.844 & 0 \\ 0 & 0 & 0 & 0 & 0 & 0.773 & 0.032 & 1.016 \\ 0 & 0 & 0 & 0 & 0 & 0 & 1.017 & 0 \end{pmatrix} \tag{12}$$

3. SIMULATION AND MEASUREMENT

Based on the above analysis, the model is built in the microwave simulation software for parametric simulation HFSS [13]. The relative dielectric constant of the ceramic dielectric material used by the filter is 20.3. Finally, the optimized dimensions of the filter are denoted in Table 1.

Figures 10(a) and 10(b) depict photographs of the processed filter. The filter has 6 tuned blind holes and 6 coupling adjustment holes on the front, which are located on different circular

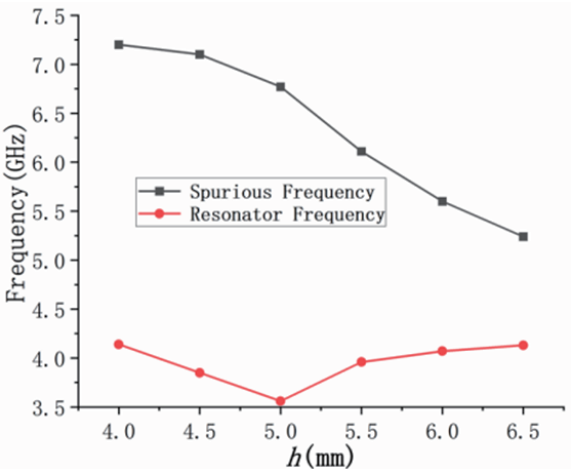

FIGURE 5. Curve of resonant frequency TM_{110} and spurious frequency with different dielectric thickness h.

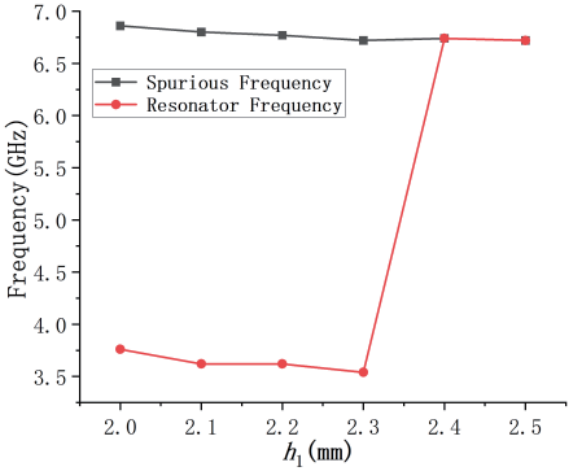

FIGURE 6. Curve of resonant frequency and spurious frequency with depth of resonant blind hole.

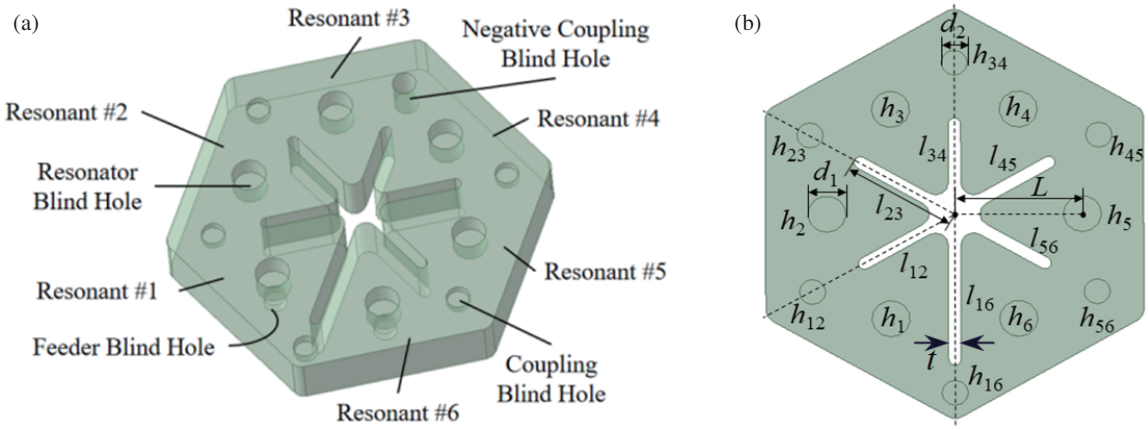

FIGURE 7. Schematic structure of the filter. (a) 3D Model. (b) Top view.

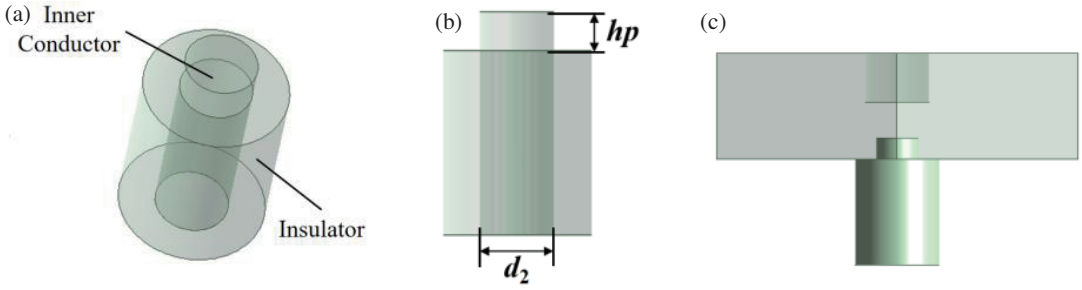

FIGURE 8. Coaxial probe. (a) 3D structure. (b) Side view. (c) Connection structure.

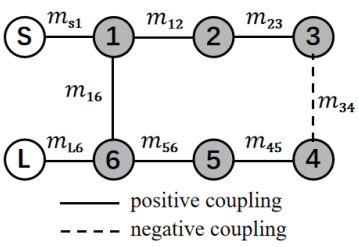

FIGURE 9. Topology structure.

arcs. On the reverse side, there are two input/output apertures with SMA interfaces welded. The entire surface is silver-plated to facilitate signal isolation.

Figure 10(c) shows the actual performance test of the filter using a vector network analyzer. As the filter is very compact, the gap between the input and output ports is very small, so a transition line needs to be connected between the transmission line and the filter, which will have some influence on the test results of the filter's performance.

TABLE 1. Filter geometry.

Parameter	Length (mm)	Parameter	Length (mm)
a	17.2	$h_2 = h_5$	2.1
h	5.0	$h_3 = h_4$	2.3
L	10.0	l_{16}	12.6
d_1	3.0	$l_{12} = l_{56}$	8.7
d_2	2.0	$l_{23} = l_{45}$	9.1
$h_1 = h_6$	2.3	l_{34}	8.0

TABLE 2. Comparison of various Indicators.

Ref	[14]	[15]	[16]	[17]	This work
Order	8	6	6	6	6
FBW (%)	5.7	5.7	5.7	6.56	5.7
IL (dB)	≤ 2	≤ 2	≤ 1.2	≤ 2	≤ 1
RL (dB)	≥ 19	≥ 17	≥ 17.5	≥ 16	≥ 16
out-of-band suppression (dB)	≥ 63	≥ 20	≥ 17	≥ 45	≥ 45
Volume (mm^3)	4788	15600	11063	4967	3843

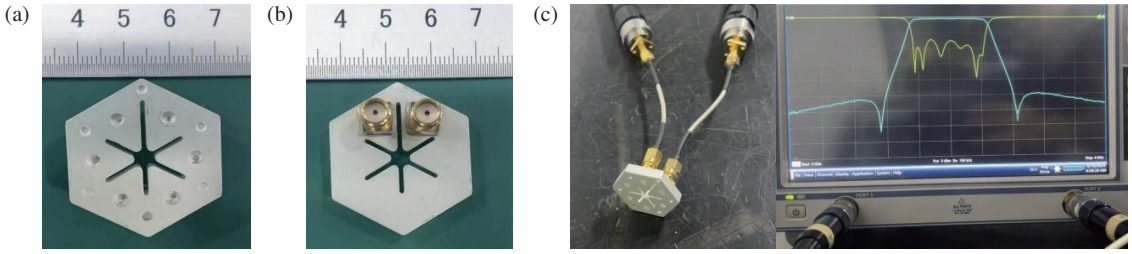

FIGURE 10. Physical object and testing. (a) Top view. (b) Bottom view. (c) VNA.

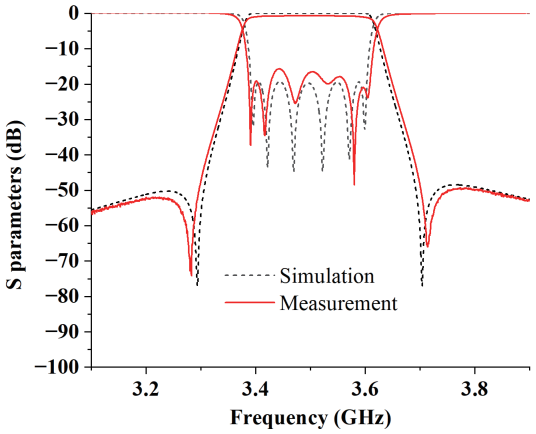

FIGURE 11. Simulated and measured results.

We can see from Fig. 11 that the designed six-cavity CDWF has a bandwidth of 0.2 GHz centered at 3.5 GHz. Within the frequency range of 3.4 GHz to 3.6 GHz, there are six poles, and the return loss exhibits suppression greater than 16 dB. Meanwhile, it contains two transmission zeros occurring at 3.28 GHz and 3.72 GHz out of the band, respectively, in which case, the filter achieves out-of-band suppression of $\geq$ 45 dB in the frequency ranges of $3 \sim 3.3$ GHz and $3.7 \sim 4$ GHz, ensuring that the filter has a good selectivity.

There are a bit difference between the simulated and actual measured results. This can be attributed to the ideal metal wall boundary conditions set in HFSS, while actual manufacturing uses a surface silver plating process. Furthermore, this discrepancy is also associated with processing accuracy and manual polishing. The proposed filter occupies a small size of 3843 mm^3.

Table 2 indicates the comparison of the designed filter and other ones [14–17]. It can be seen that our designed filter is more compact and has smaller insertion loss when working at the same center frequency.

4. CONCLUSION

Based on the equilateral triangular structure resonator, a positive hexagonal sixth-order CDWF is proposed in this paper. It has compact size and excellent insert loss. In order to verify the feasibility of the design, detailed derivations of the dimensions of the equilateral triangular resonator are carried out. The results prove that the filter has good application prospects and

important research value, and it will lead to new design possibilities in CDWFs. The proposed filter is suitable for the use in 5G base stations due to its simple structure, compact size, and excellent performance.

ACKNOWLEDGEMENT

This work is supported by the Fundamental Research Funds of China West Normal University (24kx007).

REFERENCES

[1] Dia, Y., L. Huitema, S. Bila, M. Thevenot, N. Delhote, and C. Delaveaud, "3D compact high-Q filter made of high-permittivity ceramic," in *2019 49th European Microwave Conference (EuMC)*, 304–307, Paris, France, 2019.

[2] Liu, Y., J. Pan, Q. Yang, L. Wang, and X. Ji, "A half-cut miniaturized ceramic dielectric filled cavity filter," in *2021 IEEE 5th Advanced Information Technology, Electronic and Automation Control Conference (IAEAC)*, 411–414, Chongqing, China, 2021.

[3] Du, Z., J. Pan, X. Ji, D. Yang, and X. Liu, "Ceramic dielectric-filled cavity filter," in *2020 IEEE 5th Information Technology and Mechatronics Engineering Conference (ITOEC)*, 888–891, Chongqing, China, 2020.

[4] Huang, Z., Y. Cheng, and Y. Liu, "Novel dielectric waveguide filter using isosceles right-angled triangular resonators," *Microwave and Optical Technology Letters*, Vol. 63, No. 3, 811–816, 2021.

[5] Luo, B., Z.-s. Zhan, B. Fang, and J.-b. Zhang, "A novel 5G band filter based on ceramic dielectric," in *Journal of Physics: Conference Series*, Vol. 1965, No. 1, 012060, 2021.

[6] Huang, Z., Y. Cheng, and Y. Zhang, "Circular cross-coupling dielectric waveguide filter based on 90-degree sectoral resonators," *Microwave and Optical Technology Letters*, Vol. 64, No. 2, 294–299, 2022.

[7] Lin, W., "Amplitude distribution function of several triangular waveguides," *Chinese Journal of Electronics*, Vol. 3, 36–44, 1964.

[8] Schelkonoff, S. A., *Electromagnetic Waves, Translated by Liao Shijing*, 393, Posts and Telecom Press, 1962.

[9] Zheng, Y. and Y. Zhao, "Circular monoblock dielectric resonator filter based on 60-degree sectorial resonators," in *2023 IEEE 6th International Conference on Electronic Information and Communication Technology (ICEICT)*, 259–263, Qingdao, China, Jul. 2023.

[10] Zhang, S., Z. Huang, and Y. Cheng, "A novel cross-coupled filter with triangular resonators," *Microwave and Optical Technology Letters*, Vol. 64, No. 10, 1681–1688, 2022.

[11] Yusuf, Y. and X. Gong, "Compact low-loss integration of high-Q 3-D filters with highly efficient antennas," *IEEE Transactions on Microwave Theory and Techniques*, Vol. 59, No. 4, 857–865, 2011.

[12] Zhang, S., Z. Huang, and Y. Cheng, "A novel cross-coupled filter with triangular resonators," *Microwave and Optical Technology Letters*, Vol. 64, No. 10, 1681–1688, 2022.

[13] Ansys, www.ansys.com.

[14] Meng, S., F. Liang, W. Lu, Z. Lin, Y. Yin, and R. Zhang, "Design of a microwave filter based on a novel negative coupling structure with conical through-hole," *China Communications*, Vol. 19, No. 2, 148–157, Feb. 2022.

[15] Chen, Y. and K.-L. Wu, "An all-metal capacitive coupling structure for coaxial cavity filters," in *2020 IEEE/MTT-S International Microwave Symposium (IMS)*, 583–586, Los Angeles, CA, USA, 2020.

[16] Mao, D. X., "Design of dielectric waveguide filter for 5G appli cations," Nanjing University of Posts and Telecommunications of China, Nanjing, China, 2021.

[17] Zhang, S., "Design and research of cross-coupled dielectric waveguide filter for 5G applications," Nanjing University of Posts and Telecommunications of China, Nanjing, China, 2023.